

Signal transmission in a Y-shaped one-way chain

Xiaoming Liang,^{1,*} Ming Tang,² and Huaping Lü¹

¹*School of Physics and Electronic Engineering, Jiangsu Normal University, Xuzhou 221116, China*

²*Web Sciences Center, University of Electronic Science and Technology of China, Chengdu 610054, China*

It has been found that noise plays a key role to improve signal transmission in a one-way chain of bistable systems [Zhang *et al.*, Phys. Rev. E 58, 2952 (1998)]. We here show that the signal transmission can be sharply improved without the aid of noise, if the one-way chain with a single source node is changed with two source nodes becoming a Y-shaped one-way chain. We further reveal that the enhanced signal transmission in the Y-shaped one-way chain is regulated by coupling strength, and that it is robust to noise perturbation and input signal irregularity. We finally analyze the mechanism of the enhanced signal transmission by the Y-shaped structure.

PACS numbers: 87.19.lc 05.45.Xt

The realization of transmitting weak signals over a long range is essential in engineering. Stochastic resonance has been proposed as an important mechanism to support such function, where a weak signal can be transmitted faraway without amplitude attenuation by embedding the nonlinear system that responsible for transporting the signal in a noisy environment. Subsequently, the nonlinear systems with complex structures are found to have a higher level of utilizing stochastic resonance for transmitting signals, as compared to the nonlinear systems with simple and regular structures. However, the intensity of noise is not easy to be controlled in practice, which reduces the implementation of stochastic resonance. It is an important question to ask whether there exists a specific structure by which the signal transmission can be enhanced without the help of noise. For this reason, we here propose a one-way chain with a Y-shaped structure through modifying the classical one-way chain model from having a single source node to having two disconnected source nodes. Our results show that such a slight change in the structure may enable a largely enhanced signal transmission in the one-way chain. Besides this, the enhanced signal transmission by the Y-shaped structure is much effective than by stochastic resonance. These findings may contribute to the design of highly efficient artificial devices.

I. INTRODUCTION

Exploring the relationship between structure and function of real systems has been improved markedly in recent years, as it has become clear that the impressive function of real systems is closely related to their particular structures [1–5]. Examples include the high risk of epidemic outbreak in social entities shared with small-world friendship [6], the low threshold of particle condensation in transportation network with heterogeneous structure [7], and the pathological brain states accompanied by abnormal anatomical connectivity [8]. Signal transmission over long distances is one of the most es-

sential function in nature, ranging from cell signaling in the nervous system up to human telecommunication in the engineering [9, 10], but which architecture supports an efficient and robust transmission is still not fully understood.

Early attempts at exploring the structure-function relationship of signal transmission were focused on one-way chains [11–15]. In these classical chain models, a node at one side called source node is responsible for receiving input signals, and then the source node propagates the signals to its nearest node in single direction, and so on. It has been reported that a weak signal can be transmitted along the one-way chain without amplitude damping if the chain is embedded in noisy environments [11]. Such noise-improved signal transmission is further observed in complex networks [16–22]. However, the noise-improved signal transmission relies heavily on the proper intensity of noise which it is hard to be tuned in practice. It is therefore quite important to seek a specific structure by which the transmission can be efficiently improved, instead of by the well-tuned noise.

In this paper, we propose a modified one-way chain model with a Y-shaped structure and study how such structure affects signal transmission in the chain. Unlike the classical one-way chain with a single source node, the Y-shaped one-way chain has two disconnected source nodes that receive the same input signal. We find that the Y-shaped one-way chain can maintain long-distance signal transmissions without amplitude attenuation, no matter the input signal is periodic or aperiodic. We also find that the enhanced signal transmission in the Y-shaped one-way chain is much effective than the noise-improved signal transmission in the classical one-way chain. These findings imply that even a small change in the structure might permit a hugely different performance in signal transmission, offering a good illustration of the relationship between structure and function.

II. MODEL AND METHOD DESCRIPTIONS

A Y-shaped one-way chain of $N + 1$ coupled bistable systems is shown in Fig. 1(a), whose dynamics is described as

*Electronic address: xm-liang@hotmail.com

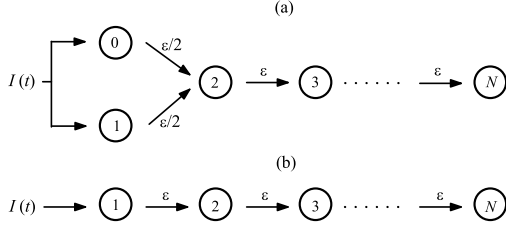


FIG. 1: Architectures of a Y-shaped one-way chain with two disconnected source nodes ($j = 0, 1$) to receive an input signal $I(t)$ in (a) and a classical one-way chain with one source node ($j = 1$) to receive the same input signal $I(t)$ in (b). ε represents the coupling strength.

follows:

$$\begin{aligned} \dot{x}_j &= x_j - x_j^3 + I(t), \quad j = 0, 1 \\ \dot{x}_2 &= x_2 - x_2^3 + \varepsilon \left(\frac{x_0 + x_1}{2} - x_2 \right), \\ \dot{x}_j &= x_j - x_j^3 + \varepsilon (x_{j-1} - x_j), \quad j = 3, \dots, N \end{aligned} \quad (1)$$

where $\dot{x}_j = x_j - x_j^3$ governs the local dynamics of node j , which has two stable fixed points $x_s = \pm 1$ and one unstable fixed point $x_u = 0$, ε denotes the coupling strength, and $I(t)$ represents the input signal receiving by the source nodes ($j = 0, 1$). To model weak signal transmissions, $I(t)$ is set as a subthreshold signal, namely, under such signal, each source node cannot jump between the two stable fixed points but oscillate around one of them. When $x_0(t) = x_1(t)$, the Y-shaped one-way chain of Eq. (1) can be viewed as a classical one-way chain with one source node, see Fig. 1(b).

To characterize signal transmission along the chain, we calculate the output of node j at the frequency ω of the input signal by [12, 18, 23, 27]

$$Q_j = \left| \frac{\omega}{n\pi} \int_0^{\frac{2n\pi}{\omega}} x_j(t) e^{i\omega t} dt \right|, \quad (2)$$

where parameter n determines the length of the integration interval. To achieve a stable result of Q_j , a large value of $n = 100$ is considered. Besides, when the input signal is aperiodic or in a noisy environment, Q_j is averaged with 100 realizations. From Eq. (2), the signal transmission along the chain is damped if $Q_j > Q_{j+1}$ for $j \geq 1$; otherwise, the transmission is enhanced if $Q_j \leq Q_{j+1}$ for $j \geq 1$. In our discussions, the chain size $N = 30$ is used, and the initial condition $x_j(0)$ of each node is randomly selected from the two stable fixed points $x_s = \pm 1$. Obviously, the two source nodes display the same dynamical behavior $x_0(t) = x_1(t)$ if their initial conditions are identical $x_0(0) = x_1(0)$, while showing different dynamical behaviors $x_0(t) \neq x_1(t)$ if their initial conditions are nonidentical $x_0(0) \neq x_1(0)$. In this regard, Eq. (1) with $x_0(0) = x_1(0)$ and with $x_0(0) \neq x_1(0)$ represents the classical one-way chain and Y-shaped one-way chain, respectively.

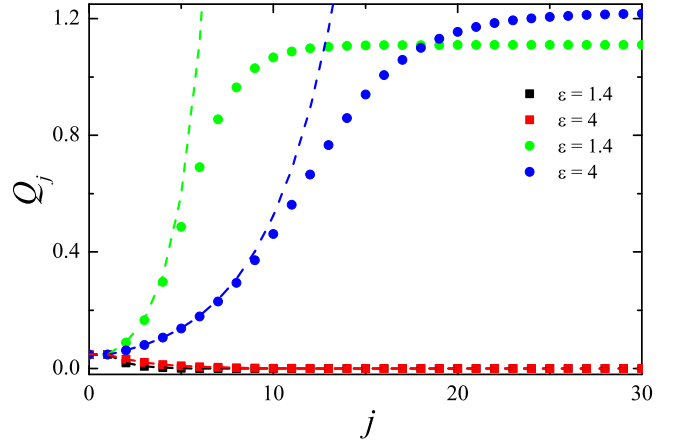


FIG. 2: (Color online) Signal transmissions of Eq. (1) with $x_0(0) = x_1(0)$ (black and red squares) and with $x_0(0) \neq x_1(0)$ (green and blue circles) at $\varepsilon = 1.4$ and $\varepsilon = 4$, respectively. Dashed lines denote the analytical predictions of Eqs. (8) and (13).

III. NUMERICAL RESULTS

A. Y-shaped structure effect

A subthreshold periodic signal $I(t) = A \sin(\omega t)$ with $\omega = \pi/5$ and $A = 0.1$ is firstly considered. Figure 2 shows the transmissions of such signal for two coupling strengths, obtaining from randomly setting the initial conditions of all the nodes. It can be observed that Q_j always takes only two distinct responses at each coupling strength: damped transmission and enhanced transmission. Our numerical results reveal that the former is achieved at $x_0(0) = x_1(0)$ while the latter is obtained at $x_0(0) \neq x_1(0)$, irrespective of the initial conditions of the other nodes. Meanwhile, Fig. 2 shows that the enhanced signal transmission obtained at $x_0(0) \neq x_1(0)$ is very sensitive to the value of coupling strength. When $\varepsilon = 1.4$, Q_j increases fast and saturates from $j = 14$. In contrast, when $\varepsilon = 4$, Q_j increases slowly but attains a higher saturated output after $j \geq 25$. Hence, the Y-shaped one-way chain (at $x_0(0) \neq x_1(0)$) has a function of enhancing signal transmission and such function is purely generated by the simple Y-shaped structure.

The above observations raise two questions: (i) How does the coupling strength impact on the enhanced output Q_j and (ii) which node has the best efficiency of enhancing signal transmission in the Y-shaped one-way chain? To answer these questions, we compare the dependencies of Q_j on ε between three nodes, see Fig. 3(a). A common feature in this figure is the same critical coupling strength $\varepsilon_c \approx 1$ below ($\varepsilon < \varepsilon_c$) or far beyond ($\varepsilon \gg \varepsilon_c$) which the output $Q_j \approx 0$. In between, the enhanced output Q_j emerges and a maximum output Q_j^M appears at an optimal coupling strength ε_j^M . Moreover, the intermediate region of ε with enhanced Q_j is expanded as j increases. During this process, the values of Q_j^M and ε_j^M are changed accordingly. As shown in Fig. 3(b), Q_j^M is an increasing function of j which satisfies

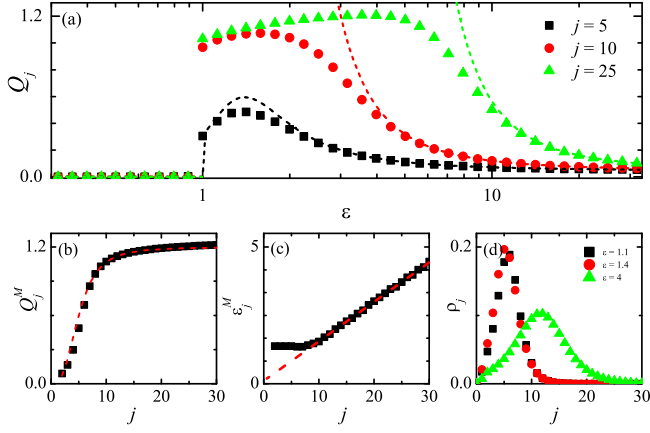


FIG. 3: (Color online) Signal transmission of Eq. (1) with $x_0(0) \neq x_1(0)$. (a) Q_j versus ε for node $j = 5$ (square), 10 (circle) and 25 (triangle). Dashed lines denote the analytical results of Eqs. (8) and (13). (b) The maximum output Q_j^M versus j with a fit line $Q_j^M = 1.2j^3/(120 + j^3)$. (c) Optimal ε_j^M versus j with a fit line $\varepsilon_j^M = 0.14(1 + j)$. (d) Transmission efficiency ρ_j versus j for $\varepsilon = 1.1$ (square), 1.4 (circle), and 4 (triangle).

$Q_j^M \approx 1.2j^3/(120 + j^3)$. In Fig. 3(c), ε_j^M seems to be a constant ($\varepsilon_j^M \approx 0.14$) before $j = 9$, and then grows with j obeying a linear relationship $\varepsilon_j^M \approx 0.14(1 + j)$. Based on these quantities, we define ρ_j to measure the signal transmission efficiency of node j as

$$\rho_j \equiv \frac{Q_j - Q_{j-1}}{j - (j-1)} = Q_j - Q_{j-1}, \quad j \geq 2 \quad (3)$$

The results of ρ_j for three coupling strengths are given in Fig. 3(d). It can be observed that ρ_j displays a bell-shaped curve at each coupling strength. In particular, when $\varepsilon = 1.1$, the curve of ρ_j has a peak at $j = 6$, suggesting that node $j = 6$ has the best efficiency of signal transmission. Interestingly, when $\varepsilon = 1.4$, the best transmission efficiency is gained by node $j = 5$ since the peak height at $j = 5$ is higher than at $j = 6$. However, when $\varepsilon = 4$, the peak of ρ_j is shifted to $j = 12$, accompanied by a decline in the peak height. The variations of ρ_j indicate that the coupling strength regulates the efficiency of signal transmission and an intermediate coupling strength enables some node to have a higher transmission efficiency.

To give a deep insight of the enhanced signal transmission, Fig. 4 shows the spectra of Q_j for nodes $j = 5, 10$, and 25 . When $\varepsilon = 1.4$, Q_5 can be seen as a delta function of ω which is zero everywhere except at the input frequency $\omega = \pi/5$, where it is a sharp peak, see Fig. 4(a). Except for the peak at $\omega = \pi/5$, Q_{10} also shows a lower peak at the harmonic frequency $\omega = 3\pi/5$, see Fig. 4(b). Such multiple peaks can be found for Q_{25} , see Fig. 4(c). In addition, when $\varepsilon = 4$, the spectra of Q_j are similar to that of $\varepsilon = 1.4$, see Figs. 4(d)-(f). The main difference is that, there are more peaks at other harmonic frequencies emerge for Q_{25} . The emergence of lower peaks at harmonic frequencies means that the output signal $x_j(t)$ is not a pure sine (cosine) wave but a sum of a set of

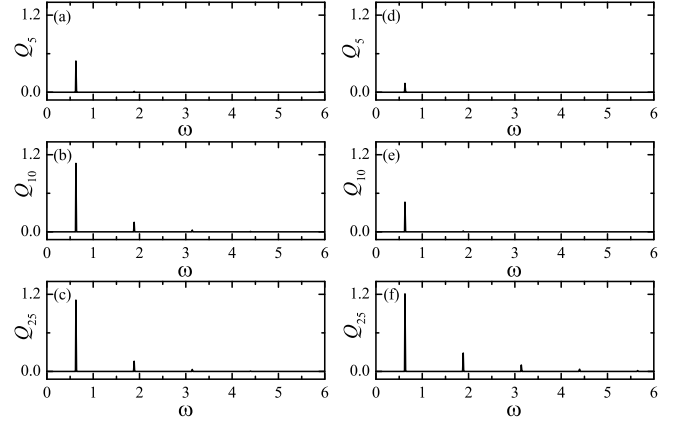


FIG. 4: Spectra of Q_j . Left panels with $\varepsilon = 1.4$: (a) $j = 5$, (b) $j = 10$, and (c) $j = 25$; Right panels with $\varepsilon = 4$: (d) $j = 5$, (e) $j = 10$, and (f) $j = 25$. Initial condition $x_0(0) \neq x_1(0)$ is used.

sine (cosine) waves. However, as the peaks at harmonic frequencies are relatively lower than the peaks at $\omega = \pi/5$, the output Q_j at the input frequency gives a reliable measurement of signal transmission.

B. Robustness to noise

Since noise is ubiquitous in nature, we examine the robustness of the enhanced signal transmission in the Y-shaped one-way chain to external noise perturbation. Hence, each bistable system in Eq. (1) becomes noisy, i.e., $\dot{x}_j = x_j - x_j^3 + \Gamma_j(t)$, where $\Gamma_j(t)$ denotes the noise perturbation. We here consider $\Gamma_j(t)$ as the white and spatially uncorrelated noise with $\langle \Gamma_j(t) \rangle = 0$ and $\langle \Gamma_j(t) \Gamma_k(t') \rangle = 2D\delta_{jk}\delta(t - t')$, where parameter D controls the intensity of noise. For a given coupling strength $\varepsilon = 4$, Fig. 5 shows the transmissions of the

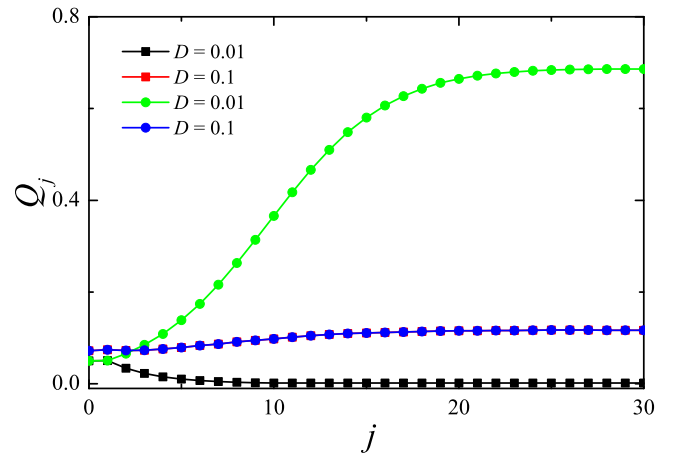


FIG. 5: (Color online) Signal transmission of Eq. (1) with $x_0(0) = x_1(0)$ (black and red square) and with $x_0(0) \neq x_1(0)$ (green and blue circles) for $D = 0.01$ and $D = 0.1$, respectively. Parameter $\varepsilon = 4$ is considered.

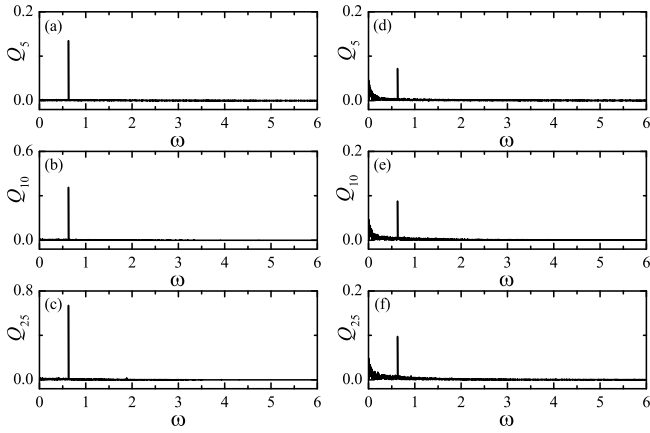


FIG. 6: Spectra of Q_j . Left panels with $D = 0.01$: (a) $j = 5$, (b) $j = 10$, and (c) $j = 25$; Right panels with $D = 0.1$: (d) $j = 5$, (e) $j = 10$, and (f) $j = 25$. Parameter $\varepsilon = 4$ and initial condition $x_0(0) \neq x_1(0)$ are used.

input signal $I(t) = A \sin(\omega t)$ in two noisy environments. In the case of $D = 0.01$, Q_j also displays two distinct responses: damped transmission at $x_0(0) = x_1(0)$ and enhanced transmission at $x_0(0) \neq x_1(0)$. In the case of $D = 0.1$, the transmission at $x_0(0) = x_1(0)$ is not damped but slightly enhanced now, which is consistent with the noise-improved signal transmission as observed in [11]. Moreover, such noise-improved transmission at $D = 0.1$ displays the same behavior to the transmission of $x_0(0) \neq x_1(0)$, implying that the enhanced signal transmission by the Y-shaped structure is reduced for large D . The phenomenon shown in Fig. 5 can be understood as follows. For small D , the two source nodes approximate $x_0(t) \approx x_1(t)$ if their initial conditions are identical $x_0(0) = x_1(0)$. Accordingly, Eq. (1) consisted of noisy bistable systems can be treated as the classical one-way chain so that it displays a similar transmission to the case of $D = 0$. For large D , the noise perturbation is sufficient that it can trigger the source nodes jump between their two stable fixed points. Therefore, the signal transmission is independent of the initial conditions of the source nodes, which results in the same transmission between $x_0(0) = x_1(0)$ and $x_0(0) \neq x_1(0)$.

Fixed $\varepsilon = 4$, we explore the dependency of Q_j on ω for three nodes chosen from Fig. 5. The results are displayed in Fig. 6. For $D = 0.01$, the curve of Q_j can be viewed as a delta function with a sharp peak at the input frequency $\omega = \pi/5$, see Figs. 6(a)-(c). For $D = 0.1$, Q_j also resembles a delta function except small $\omega \approx 0$ at which $Q_j > 0$, see Figs. 6(d)-(f). The common peak at $\omega = \pi/5$ shown in Fig. 6 suggests that the input frequency is the main frequency of the output signals and thus the output Q_j at $\omega = \pi/5$ is the dominant output.

In addition, the same transmission at large D shown in Fig. 5 motivates us to figure out the critical noise intensity at which the signal transmission is irrelevant to the initial conditions of the source nodes. To this end, we compare the evolutions of Q_j with D between $x_0(0) \neq x_1(0)$ and $x_0(0) = x_1(0)$ for

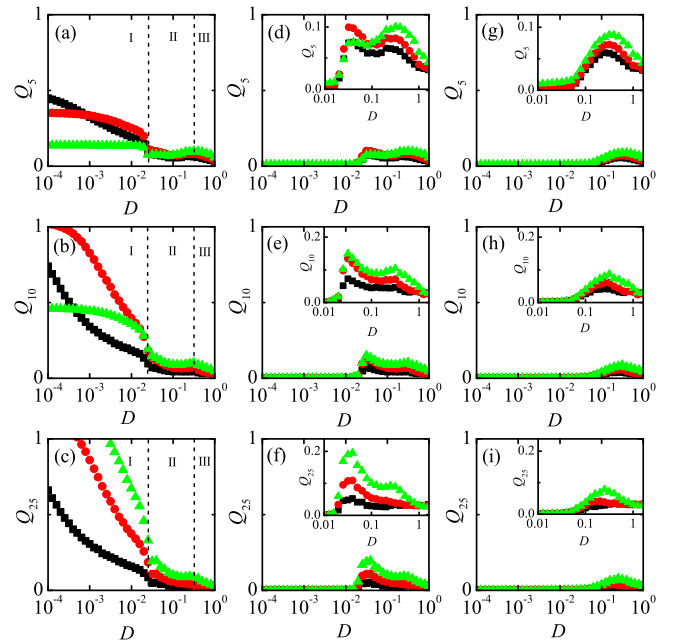


FIG. 7: (Color online) Signal transmission of Eq. (1) at $\varepsilon = 1.4$ (square), 2 (circle), and 4 (triangle), respectively. Upper panels for $j = 5$: (a) $x_0(0) \neq x_1(0)$, (b) $x_0(0) = x_1(0)$, (c) $x_0(0) = x_1(0)$ and $\Gamma_0(t) = \Gamma_1(t)$; Middle panels for $j = 10$: (d) $x_0(0) \neq x_1(0)$, (e) $x_0(0) = x_1(0)$, (f) $x_0(0) = x_1(0)$ and $\Gamma_0(t) = \Gamma_1(t)$; Lower panels for $j = 25$: (d) $x_0(0) \neq x_1(0)$, (e) $x_0(0) = x_1(0)$, (f) $x_0(0) = x_1(0)$ and $\Gamma_0(t) = \Gamma_1(t)$. Insets are the enlarged views of signal transmissions.

several values of j and ε , see Fig. 7. When $x_0(0) \neq x_1(0)$, Q_j decays with D except a slight rise around $D \approx 0.3$, see Figs. 7(a)-(c). When $x_0(0) = x_1(0)$, Q_j suddenly increases from $D \approx 0.02$ until attaining a local maximum at $D \approx 0.03$, exhibiting the same performance to the case of $x_0(0) \neq x_1(0)$ for large D , see Figs. 7(d)-(f). When j or ε varies, the value of $D \approx 0.03$ remains constant, which indicates that $D \approx 0.03$ is the critical noise intensity at which the signal transmission in the Y-shaped one-way chain is not sensitive to the initial conditions of the source nodes. Besides, Figs. 7(d)-(f) (insets) also show that Q_j may exhibit two resonant peaks for suitable ε , forming double resonant-like phenomena. Further, Figs. 7(g)-(i) (insets) depict the evolutions of Q_j for the classical one-way chain, by setting $x_0(0) = x_1(0)$ and $\Gamma_0(t) = \Gamma_1(t)$ in Eq. (1). In these figures, Q_j shows a resonant-like dependency on D for each pair of j and ε , where the resonant peak is at $D \approx 0.3$. When $D > 0.3$, Q_j exhibits a similar evolution to the cases of $x_0(0) \neq x_1(0)$ and $x_0(0) = x_1(0)$. This implies that $D \approx 0.3$ is another critical noise intensity, above which the difference in signal transmission between the Y-shaped one-way chain and classical one-way chain is small. Making use of these two critical intensities, we may divide the signal transmission in the Y-shaped one-way chain into three regions: region I ($D \leq D_1 = 0.03$), region II ($D_1 < D < D_2 = 0.3$), and region III ($D \geq D_2$) [see Figs. 7(a)-(c)]. Specifically, region I corresponds to the Y-shaped structure-improved transmission, region II cor-

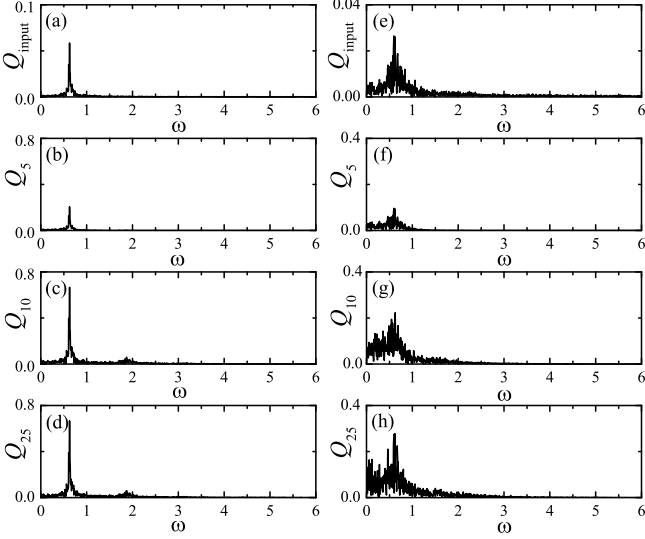


FIG. 8: Spectra of Q_j . Left panels with $T = 0.01$: (a) Q_{input} , (b) $j = 5$, (c) $j = 10$, and (d) $j = 25$; Right panels with $T = 0.1$: (e) Q_{input} , (f) $j = 5$, (g) $j = 10$, and (h) $j = 25$. Parameter $\varepsilon = 2$ and $x_0(0) \neq x_1(0)$ are set.

responds the structure-noise-improved transmission, and region III corresponds the noise-improved transmission, respectively. Among them, the Y-shaped structure-improved transmission (region I) is robust to noise perturbation, especially at large ε since the decay rate is slow. In addition, the Y-shaped structure-improved transmission is much more effective than the noise-improved transmission.

C. Robustness to signal irregularity

The actual signals are usually irregular ones, it is necessary to check the robustness of the Y-shaped structure-improved transmission to input signal irregularity. Here the irregular input signal is generated by setting the periodic signal with a time-varying initial phase $\varphi(t)$, i.e., $I(t) = A \sin(\omega t + \varphi(t))$ [24]. For simplicity, the initial phase $\varphi(t)$ is set to be varied as a Wiener process. Thus, $\dot{\varphi}(t) = \zeta(t)$ is a Gaussian white noise with $\langle \zeta_i(t) \rangle = 0$ and $\langle \zeta(t)\zeta(t') \rangle = 2T\delta(t - t')$. When $T > 0$, the periodic signal $I(t) = A \sin(\omega t)$ becomes an aperiodic signal and its regularity decreases with T . To illustrate it, we show the output spectrum of the aperiodic signal at $T = 0.01$ [see Fig. 8(a)] and at $T = 0.1$ [see Fig. 8(e)], respectively. In both spectra, there is a highest peak at $\omega \approx \pi/5$, where the peak height is lower and peak width is wider at $T = 0.1$, demonstrating that the regularity of the aperiodic signal is decreased with T . We next investigate whether these two aperiodic signals can be effectively transmitted in the Y-shaped one-way chain. Fixing $\varepsilon = 2$, Figs. 8(b)-(d) depict the output spectra for three nodes $j = 5, 10$, and 25 at $T = 0.01$. It is obvious that each output spectrum can be considered as an enlarged version of Fig. 8(a), where the output spectra of Q_{10} and Q_{25} show larger enlarged ratios than that

of Q_5 . Similarly, such enlarged versions can also be observed in Figs. 8(e)-(h) for the case of $T = 0.1$. Comparing with that of $T = 0.01$, the enlarged ratio and fidelity are reduced at $T = 0.1$. From these observations, it can be concluded that the Y-shaped structure-improved transmission works well for irregular signals.

IV. ANALYTICAL RESULTS

We now analyze the underlying mechanism of the Y-shaped structure-improved signal transmission. To avoid the effect of noise, we only discuss Eq. (1) subjected to a periodic input signal ($T = 0$) in absence of noise ($D = 0$). Because the input signal $I(t) = A \sin(\omega t)$ is subthreshold, the source nodes oscillate with small amplitudes around the stable fixed points, their solutions can be approximately obtained as [23, 25, 26]

$$x_j(t) \approx x_j(0) + A_1 \sin(\omega t + \varphi_1), \quad j = 0, 1 \quad (4)$$

where $x_j(0) = \pm 1$ depending on the initial condition, $A_1 = A/\sqrt{\omega^2 + 4}$, and φ_1 denotes some phase shift.

A. Case 1: Two source nodes with the same initial condition

When $x_0(0) = x_1(0)$, the dynamical equation of node $j = 2$ becomes

$$\dot{x}_2 = (1 - \varepsilon)x_2 - x_2^3 + \varepsilon x_1(0) + \varepsilon A_1 \sin(\omega t + \varphi_1). \quad (5)$$

Without the periodic signal $\varepsilon A_1 \sin(\omega t + \varphi_1)$, x_2 has three fixed points for $\varepsilon \leq 1/4$: $x_1(0)$ and $-1/2 \pm \sqrt{1 - 4\varepsilon}/2$ in which $x_1(0)$ and $-1/2 - \sqrt{1 - 4\varepsilon}/2$ are stable fixed points while $-1/2 + \sqrt{1 - 4\varepsilon}/2$ is unstable; for $\varepsilon > 1/4$, x_2 has one stable fixed point $x_1(0)$. When ε is not great, the signal $\varepsilon A_1 \sin(\omega t + \varphi_1)$ is subthreshold, the solutions of the node $j = 2$ approximate

$$x_2(t) \approx x_1(0) + \frac{\varepsilon A_1}{\sqrt{\omega^2 + (2 + \varepsilon)^2}} \sin(\omega t + \varphi_2)$$

and

$$x_2(t) \approx \frac{-1 - \sqrt{1 - 4\varepsilon}}{2} + \frac{\varepsilon A_1}{\sqrt{\omega^2 + (\frac{1}{4} - \varepsilon)^2}} \sin(\omega t + \varphi_2),$$

where φ_2 is some phase shift. When $\varepsilon \approx 1/4$, the latter solution indicates a larger oscillation around $-1/2 - \sqrt{1 - 4\varepsilon}/2$ than the former around $x_1(0)$. However, the stability of the fixed point $-1/2 - \sqrt{1 - 4\varepsilon}/2$ decreases as ε approaches $1/4$, the large oscillation is thus unsustainable and it will move to the vicinity of $x_1(0)$, leading to a small oscillation governed by the former solution. Inserting $x_2(t)$ into the equation of node $j = 3$, we can obtain the stable fixed points of the node $j = 3$ as well as the subsequent nodes by repeatedly using the same method. We find that these nodes possess the same stable fixed point 1 or -1 , depending on $x_1(0) = 1$ or

$x_1(0) = -1$. In this way, the dynamical equation of node $j \geq 3$ can be written as

$$\dot{x}_j \approx (1-\varepsilon)x_j - x_j^3 + \varepsilon x_1(0) + \varepsilon A_{j-1} \sin(\omega t + \varphi_{j-1}), \quad (6)$$

where $\varepsilon A_{j-1} \sin(\omega t + \varphi_{j-1})$ denotes the signal from node $j-1$ and φ_{j-1} represents some phase shift. When the signal $\varepsilon A_{j-1} \sin(\omega t + \varphi_{j-1})$ is subthreshold, the solution of Eq. (6) approximately satisfies

$$x_j(t) \approx x_1(0) + \frac{\varepsilon A_{j-1}}{\sqrt{\omega^2 + (2+\varepsilon)^2}} \sin(\omega t + \varphi_j) \approx x_1(0) + \left(\frac{\varepsilon}{\sqrt{\omega^2 + (2+\varepsilon)^2}} \right)^{j-1} A_{j-1} \sin(\omega t + \varphi_j) \quad (7)$$

with some phase shift φ_j . Inserting this solution into Eq. (2), the output Q_j is given by

$$Q_j \approx A_1 \left(\frac{\varepsilon}{\sqrt{\omega^2 + (2+\varepsilon)^2}} \right)^{j-1}. \quad (8)$$

Eq. (8) satisfies the condition $Q_j > Q_{j+1}$ for $j \geq 1$, thereby supporting the damped transmission of Eq. (1) at $x_0(0) = x_1(0)$.

On the other hand, the damped transmission at $x_0(0) = x_1(0)$ can be explained by the overdamped motion of a particle in a potential and periodic forcing [28]. For this reason, the potential in Eq. (6) is $V(x) = -(1-\varepsilon)x^2/2 + x^4/4 + \varepsilon x_1(0)x$ and the periodic forcing is $\varepsilon A_{j-1} \sin(\omega t + \varphi_{j-1})$. When $\varepsilon > 0$, $V(x)$ is an asymmetrical potential and its asymmetry is determined by the value of ε . For illustration, Figs. 9(a)-(c) display the potential $V(x)$ for $\varepsilon = 0.2, 0.9$ and 1.4 . When $\varepsilon = 0.2$, $V(x)$ has two wells, where the well located at $x = 1$ (or $x = -1$) is deeper than the other one at $x \approx 0.7$ (or $x \approx -0.7$), see Fig. 9(a). This indicates that the large oscillations around $x = 1$ (or $x = -1$) are more stable. When ε is increased to 0.9 , $V(x)$ turns into an V-shaped potential with a single well at $x = 1$ (or $x = -1$), see Fig. 9(b). As shown in Fig. 9(c), further increasing ε to 1.4 will result in a more steep V-shaped potential. Clearly, under the same forcing of $\varepsilon A_{j-1} \sin(\omega t + \varphi_{j-1})$, the asymmetrical potential $V(x)$ of $\varepsilon = 0.2$ allows the particle to generate a relatively large oscillation inside it in contrast to the potentials of $\varepsilon = 0.9$ and $\varepsilon = 1.4$. However, as $\varepsilon A_{j-1} \sin(\omega t + \varphi_{j-1})$ is weak and the motion is overdamped, the oscillation around $x = 1$ (or $x = -1$) gets even smaller ($A_j < A_{j-1}$). Altogether, the transmission of Eq. (1) decreases with j and ε when $x_0(0) = x_1(0)$.

B. Case 2: Two source nodes with different initial conditions

When $x_0(0) \neq x_1(0)$, Eq. (5) can be rewritten as

$$\dot{x}_2 = (1-\varepsilon)x_2 - x_2^3 + \varepsilon A_1 \sin(\omega t + \varphi_1). \quad (9)$$

Without the periodic signal $\varepsilon A_1 \sin(\omega t + \varphi_1)$, x_2 has two stable fixed points $\pm\sqrt{1-\varepsilon}$ for $\varepsilon < 1$ and has one stable fixed point 0 for $\varepsilon \geq 1$. For a subthreshold signal

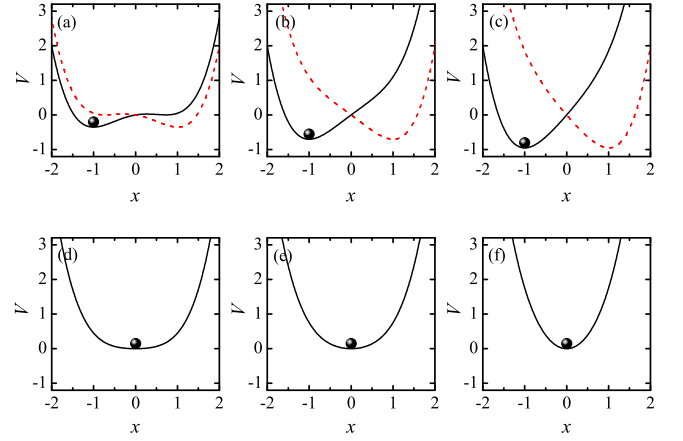


FIG. 9: (Color online) Potential $V(x)$ for different ε . Upper panels for $V(x) = -(1-\varepsilon)\frac{x^2}{2} + \frac{x^4}{4} - \varepsilon x_1(0)x$: (a) $\varepsilon = 0.2$, (b) $\varepsilon = 0.9$, and (c) $\varepsilon = 1.4$. Solid lines correspond to $x_1(0) = 1$ and the dashed lines correspond to $x_1(0) = -1$. Lower panels for $V(x) = -(1-\varepsilon)\frac{x^2}{2} + \frac{x^4}{4}$: (d) $\varepsilon = 1.4$, (e) $\varepsilon = 2$, and (f) $\varepsilon = 4$.

$\varepsilon A_1 \sin(\omega t + \varphi_1)$, the solutions of $x_2(t)$ approximate

$$x_2(t) \approx \pm\sqrt{1-\varepsilon} + \frac{\varepsilon A_1}{\sqrt{\omega^2 + 4(1-\varepsilon)^2}} \sin(\omega t + \varphi'_2)$$

and

$$x_2(t) \approx \frac{\varepsilon A_1}{\sqrt{\omega^2 + (1-\varepsilon)^2}} \sin(\omega t + \varphi'_2),$$

where φ'_2 is some phase shift. Based on the solutions of $x_2(t)$, we can acquire the stable fixed points of the subsequent nodes $j \geq 3$. We find that the stable fixed points of these nodes are ± 1 for $\varepsilon < 1$ and 0 for $\varepsilon \geq 1$. In the former case, the dynamical equation of node $j \geq 3$ can be rewritten as

$$\dot{x}_j \approx (1-\varepsilon)x_j - x_j^3 + \varepsilon x_1(0) + \varepsilon A_{j-1} \sin(\omega t + \varphi'_{j-1}), \quad (10)$$

where φ'_{j-1} is some phase shift. Eq. (10) has the same form as Eq. (6), so their solutions and the corresponding outputs are similar. This means the signal transmission is damped for $\varepsilon < 1$ no matter the initial condition is $x_0(0) = x_1(0)$ or $x_0(0) \neq x_1(0)$. In the latter case, i.e., $\varepsilon \geq 1$, the dynamics equation of node $j \geq 3$ is

$$\dot{x}_j \approx (1-\varepsilon)x_j - x_j^3 + \varepsilon A_{j-1} \sin(\omega t + \varphi'_{j-1}). \quad (11)$$

Its solution is

$$x_j(t) \approx \left(\frac{\varepsilon}{\sqrt{\omega^2 + (1-\varepsilon)^2}} \right)^{j-1} A_1 \sin(\omega t + \varphi'_j), \quad (12)$$

where φ'_j is some phase shift. Inserting Eq. (12) into Eq. (2), the output is

$$Q_j \approx A_1 \left(\frac{\varepsilon}{\sqrt{\omega^2 + (1-\varepsilon)^2}} \right)^{j-1}. \quad (13)$$

Eq. (13) satisfies the condition $Q_j \leq Q_{j+1}$ for $j \geq 1$, which coincides with the enhanced signal transmissions at $x_0(0) \neq x_1(0)$. In Fig. 2 and Fig. 3(a), we compare the analytical results of Eqs. (8) and (13) with the numerical results and find a good agreement between them for small j . The reason is that, the above analyses are based on the perturbation theory, i.e., assuming x_j oscillates around the stable fixed point with a small amplitude. Because the oscillation of x_j is weak for small j , the theory gives a better approximation to x_j as well as Q_j . In addition, from Eq. (13), the optimal ε_j^M can be derived as $\varepsilon_j^M = 1 + \omega^2 \approx 1.4$, which fits well with the numerical results ($j \leq 9$) shown in Fig. 3(b).

Analogously, the enhanced signal transmission at $x_0(0) \neq x_1(0)$ and $\varepsilon \geq 1$ can also be understood by the overdamped motion of a particle in a potential and periodic forcing. As shown in Eq. (11), the periodic forcing is $\varepsilon A_{j-1} \sin(\omega t + \varphi_{j-1})$, and the potential is $V(x) = -(1 - \varepsilon)x^2/2 + x^4/4$ which is a symmetrical function with a minimum at $x = 0$. In Fig. 9(d), the potential $V(x)$ for $\varepsilon = 1.4$ is plotted. It is a U-shaped curve with a flat bottom, which is quite different from the V-shaped well shown in Fig. 9(c). In addition, Fig. 9(e) plots the potential $V(x)$ for $\varepsilon = 2$. It can be seen that the bottom of the U-shaped $V(x)$ becomes narrow and such narrow U-shaped potential transforms into a V-shaped curve as $\varepsilon = 4$, see Fig. 9(f). In contrast, the U-shaped potential $V(x)$ can permit the particle to gain a wider oscillation inside it than the V-shaped potentials. This explains why the signal transmission is largely enhanced at $x_0(0) \neq x_1(0)$ and $\varepsilon = 1.4$.

C. Mechanisms of resonant-like phenomena

We finally analyze the mechanism of the resonant-like phenomena shown in Fig. 7. Firstly, we explain the single resonant-like dependency for the classical one-way chain with one source node, i.e., $x_0(0) = x_1(0)$ and $\Gamma_0(t) = \Gamma_1(t)$ are set in Eq. (1). When $D = 0$, the oscillation of the source node is small, restricting in one of the two stable fixed points. When D is increased to $D = 0.03$, the oscillation of the source node can jump to the other stable fixed point by noise perturbation, see Fig. 10(a). Because the perturbations are not sufficient, the jumping rate is small and the oscillation may stay there for a long time until the next jumping. Thus the oscillation of the source node is still small at $D = 0.03$. Continue increasing D to $D = 0.05$, the jumping rate between the two stable fixed points is obviously improved, which increases the oscillation amplitude, see Fig. 10(b). When $D = 0.3$, the jumping rate is sharply improved, so the oscillation is no longer centered on the stable fixed points $x_s = \pm 1$ but on $x_u = 0$, see Fig. 10(c). However, further increase in D will increase the randomness of the oscillation (not shown here). Considering all of these factors, the source node can only generate a large output at $D = 0.3$, showing a resonant peak over there. Through one-way coupling, the output of the source node will propagate to the subsequent nodes ($j \geq 2$), which results in the stochastic resonance phenomena as observed in Figs. 7(g)-(i).

Secondly, we explain the double resonant-like dependency

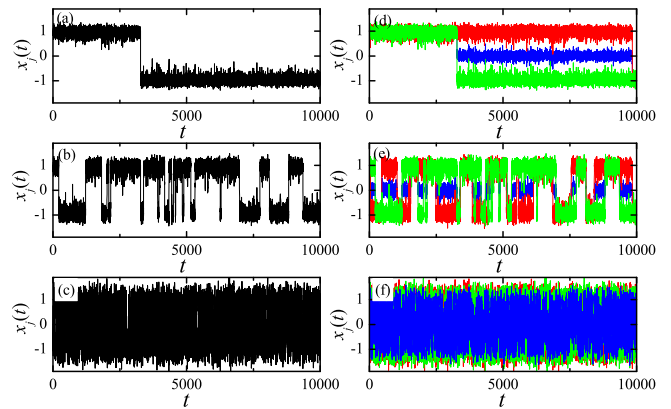


FIG. 10: (Color online) Time series $x_j(t)$ of the source node(s). Left panels for one source node: (a) $D = 0.03$, (b) $D = 0.05$, and (c) $D = 0.3$; Right panels for two source nodes with given the same initial condition $x_0(0) = x_1(1)$: (d) $D = 0.03$, (e) $D = 0.05$, and (f) $D = 0.3$. Red and green lines denote $x_j(t)$ of the two source nodes, blue lines denote the their collective dynamics $(x_0(t) + x_1(t))/2$.

for the Y-shaped one-way chain with $x_0(0) = x_1(0)$. As mentioned above, when $D = 0.03$, there is a small probability that a single source node may jump to the other stable fixed point, remaining there for a long time until it jumps back to the initial fixed point. In this way, the two source nodes in the Y-shaped one-way chain may occasionally oscillate in different stable fixed points for long time intervals, although given the same initial condition $x_0(0) = x_1(0)$, see Fig. 10(d). Considering that the signal transmission is largely enhanced if the two source nodes oscillate in different stable fixed points [see Sec. IV B], the transmission in the Y-shaped one-way chain will be sometimes largely enhanced at $D = 0.03$. By increasing D to $D = 0.05$, the time intervals for the two source nodes simultaneously oscillating at different fixed points reduce dramatically [see Fig. 10(e)], indicating a decrease in signal transmission. These are the reasons why Q_j shows the first local peak at $D = 0.03$. When D is increased to $D = 0.3$, there is no obvious interval between two continuous jumps, see Fig. 10(f). During this process, the collective behavior of the two source nodes $(x_0(t) + x_1(t))/2$ is analogous to the individual $x_0(t)$ or $x_1(t)$, i.e., the two source nodes can be seen as a single one. This analogy in dynamics implies that the Y-shaped one-way chain shows a similar signal transmission to that of the classical one-way chain for large D . As a result, the signal transmission in the Y-shaped one-way chain is also largely enhanced at $D = 0.3$, resulting in the second peak over there. Obviously, both the single and double resonant-like dependencies are the stochastic resonance phenomena, since the signal transmissions are improved by noise. However, as the specific Y-shaped structure allows the two source nodes oscillate in distinct fixed points for small noise, we thus refer the enhanced signal transmission in the region $0.03 < D < 0.3$ as structure-noise-improved transmission [see Figs. 7(d)-(f)].

V. SUMMARY

In conclusions, we have studied the signal transmission in a Y-shaped one-way chain and found an extraordinarily of such specific structure to improve signal transmission. We have also studied the robustness of the Y-shaped structure-improved transmission to the noise perturbation and input signal regularity. We hope our findings may contribute to understand the structure-function relationship of real systems and be useful to design highly efficient artificial devices, such as switchers and amplifiers.

ACKNOWLEDGMENTS

X.L. was supported by the NNSF of China under Grant No. 11305078, the Research Fund of Jiangsu Normal University under Grant No. 12XLR028, and the Priority Academic Program Development of Jiangsu Higher Education Institutions (PAPD). M.T. was supported by the NNSF of China under Grant No. 11105025. H.L. was supported by the NNSF of China under Grant No. 11175150.

-
- [1] S. Boccaletti, V. Latora, Y. Moreno, M. Chavez, and D.-U. Hwang, *Phys. Rep.* **424**, 175 (2006).
 - [2] R. Albert and A. Barabási, *Rev. Mod. Phys.* **74**, 47 (2002).
 - [3] M. E. J. Newman, *SIAM Review* **45**, 167 (2003).
 - [4] O. V. Popovych, S. Yanchuk, and P. A. Tass, *Phys. Rev. Lett.* **107**, 228102 (2011).
 - [5] Z. Liu, B. Li, and Y.-C. Lai, *EPL* **98**, 20005 (2012).
 - [6] M. E. J. Newman, *Phys. Rev. E* **61**, 5678 (2000).
 - [7] M. Tang and Z. Liu, *Physica A* **387**, 1361 (2008).
 - [8] E. Bullmore and O. Sporns, *Nat. Rev. Neurosci.* **10**, 186 (2009).
 - [9] A. Kumar, S. Rotter, and A. Aertsen, *Nat. Rev. Neurosci.* **11**, 615 (2010).
 - [10] N. J. McCullen, T. Mullin, and M. Golubitsky, *Phys. Rev. Lett.* **98**, 254101 (2007).
 - [11] Y. Zhang, G. Hu, and L. Gammaitoni, *Phys. Rev. E* **58**, 2952 (1998).
 - [12] A. A. Zaikin, J. García-Ojalvo, L. Schimansky-Geier, and J. Kurths, *Phys. Rev. Lett.* **88**, 010601 (2001).
 - [13] C. Yao and M. Zhan, *Phys. Rev. E* **81**, 061129 (2010).
 - [14] Z. Liu, *EPL* **100**, 60002 (2012).
 - [15] J. Wang and Z. Liu, *EPL* **102**, 10003 (2013).
 - [16] Q. Wang, Q. Lu, and G. Chen, *EPL* **77**, 10004 (2007).
 - [17] M. Perc, *Phys. Rev. E* **76**, 066203 (2007).
 - [18] M. Perc, *Phys. Rev. E* **78**, 036105 (2008).
 - [19] M. Perc and M. Gosak, *New J. Phys.* **10**, 053008 (2008).
 - [20] M. Ozer, M. Perc, and M. Uzuntarla, *Phys. Lett. A* **373**, 964 (2009).
 - [21] X. Sun, M. Perc, Q. Lu, and J. Kurths, *Chaos* **20**, 033116 (2010).
 - [22] Z. Liu and T. Munakata, *Phys. Rev. E* **78**, 046111 (2008).
 - [23] X. Liang, Z. Liu, and B. Li, *Phys. Rev. E* **80**, 046102 (2009).
 - [24] X. Liang, L. Zhao, and Z. Liu, *Phys. Rev. E* **84**, 031916 (2011).
 - [25] J. A. Acebró, S. Lozano, and A. Arenas, *Phys. Rev. Lett.* **99**, 128701 (2007).
 - [26] X. Liang, L. Zhao, and Z. Liu, *Chaos* **22**, 023128 (2012).
 - [27] X. Liang, S. Yanchuk, and L. Zhao, *Phys. Rev. E* **88**, 012910 (2013).
 - [28] L. Gammaitoni, P. Hänggi, P. Jung, and F. Marchesoni, *Rev. Mod. Phys.* **70**, 223 (1998).